JOURNAL OF GEOPHYSICAL RESEARCH, VOL. 100, NO. C7, PAGES 13,179–13,192, JULY 15, 1995

The average cosine due to an isotropic light source in the ocean

R. A. Maffione
Applied Electromagnetics and Optics Laboratory, SRI International, Menlo Park, California

J. S. Jaffe
Marine Physical Laboratory, Scripps Institution of Oceanography, La Jolla, California

Abstract. The average cosine $\bar{\mu}$ of the light field created by an isotropic point source (IPS) embedded in a homogeneous ocean is investigated with a Monte Carlo model. Two volume scattering functions (VSFs) are used in the model, taken from Petzold (1972), to compute the radiance distributions at various distances from the source. The simulated radiance distributions are compared with measurements of the point spread function made at Lake Pend Oreille, Idaho, during the 1992 optical closure experiment. An analytic model is presented for $\bar{\mu}$ which is valid to at least 15 optical lengths from the source. The model shows that the mean light path, derived from $\bar{\mu}$, is a strong function of the single scattering albedo and the VSF. We found that errors in estimating the absorption coefficient by neglecting the increase in the mean light path, which is due to scattering, vary between 5% and 12% for nearly all natural waters. A mathematical proof is given that $\bar{\mu} \rightarrow 1$ as the distance to the IPS goes to zero. An analytic expression is derived for $\bar{\mu}$ close to a finite diffuse-isotropic source which shows that $\bar{\mu}$ approaches one as the distance decreases, but at extremely close distances, $\bar{\mu} \rightarrow 1/2$ as the distance to the surface of the source goes to zero. At distances beyond one attenuation length, for finite sources small compared to an attenuation length, $\bar{\mu}$ behaves essentially as it would for a point source. An asymptotic model for $\bar{\mu}$ as a function of the single scattering albedo is given with coefficients that depend on the VSF. Model results and comparisons with measured PSFs reveal the surprising result that the light field from an embedded isotropic point source in the ocean does not exhibit asymptotic behavior as far as 15 attenuation lengths from the source.

Introduction

The light field due to an isotropic point source (IPS) embedded in the ocean is interesting to study because this light field, under suitable mathematical transformations, provides a wealth of information about the optical properties of the water. To the extent that the ocean may be thought of as a linear optical medium, the radiance distribution at each point in the water due to an embedded IPS is the optical impulse response (OIR) of the medium. The OIR is commonly referred to as the point spread function (PSF), although the PSF for imaging systems is usually defined as the (output) radiance distribution due to a point Lambertian source. In this case, the transformation of any input light field by the optical system is given by the spatial convolution of the input light field with the OIR. The ocean laser community defines the PSF similarly because of its equivalence to the beam spread function (BSF), which is the angular irradiance distribution due to a unidirectional light beam [*Mertens and Replogle*, 1977]. In the small-angle range (less than 10°), both the isotropic- and Lambertian-source defined PSFs are empirically nearly equal. In general, however, they should be distinguished.

Paper number 95JC00461.
0148-0227/95/95JC-00461$05.00

Aside from its powerful use as the OIR of an optical medium, the light field due to an IPS embedded in the ocean can, in principle, be mathematically transformed to yield all of the inherent optical properties (IOPs) of the medium. *Sorenson and Honey* [1968], for example, conjectured that the beam attenuation, volume absorption, and backward scattering coefficients can all be determined from radiance and irradiance measurements of an IPS. Sorenson and Honey's conjectures were experimentally verified as good approximations [*Honey and Maffione*, 1992; *Maffione*, 1993; *Maffione and Honey*, 1991; *Maffione et al.*, 1991, 1993]. *Wells* [1969] first presented the transformation of the PSF to the volume scattering function (VSF) in the small-angle approximation. Although Wells' transformation to the VSF has yet to be experimentally tested in the sense of closure, it was recently numerically tested and found to be accurate within the small-angle scattering limit up to about six attenuation lengths [*Jaffe*, 1995].

To the authors' knowledge, the only known exact transformation to an inherent optical property from an IPS light field was presented by *Maffione et al.* [1993]. They showed that the absorption coefficient a could be obtained exactly from the scalar irradiance and divergence of the vector irradiance by simply transforming *Gershun*'s [1936] equation to spherical coordinates. For homogeneous water the problem reduces to one spatial coordinate, the radial distance r from the source, and the resulting solution is given by

$$a = \bar{\mu}_r(r)\left[K_r(r) - \frac{2}{r}\right], \tag{1}$$

where

$$K_r(r) = \frac{-1}{E_r(r)}\frac{dE_r(r)}{dr} \tag{2}$$

is defined as the radial attenuation coefficient for net radial irradiance E_r and

$$\bar{\mu}_r(r) = \frac{E_r(r)}{E_0(r)} \tag{3}$$

is defined as the radial average cosine. The net radial irradiance is the difference between the irradiance flowing away from the source and the irradiance flowing in toward the source due to scattering. E_r is analogous to the vertical component of the vector irradiance in a Cartesian coordinate system; E_0 is the scalar irradiance. It is understood that all quantities are spectral. Henceforth, the subscript r and the adjective radial will be omitted. Comparing (1) to the analogous form of Gershun's equation,

$$a = \bar{\mu}(r)K(r) \tag{4}$$

reveals that Gershun's equation is actually a special case of the more general form (1) when $r \to \infty$. In other words, Gershun's equation is the far-field approximation where the electromagnetic waves are considered plane waves and horizontal gradients in the electromagnetic field are neglected.

The average cosine $\bar{\mu}$ is an apparent optical property (AOP) since it depends on the structure of the light field. The importance of Gershun's equation (4) is that the product of the average cosine with another AOP, the irradiance attenuation coefficient K, yields the absorption coefficient, an IOP which depends only on the physical properties of the water. In the more general case (1), the absorption coefficient is given by the product $\bar{\mu}K$ minus the geometric reduction due to the spherically expanding light field of an IPS, but this geometric term also contains $\bar{\mu}$. Thus the average cosine is fundamental to understanding how the ocean transforms the light field and how that transformation is related to the absorption of light by the water.

In this paper we investigate the behavior of $\bar{\mu}$ from the radiance distribution due to an IPS embedded in the ocean using a Monte Carlo (MC) model. The computed radiance distributions are compared with PSFs that were measured in Lake Pend Oreille during the Office of Naval Research (ONR) sponsored optical closure experiment in April–May 1992 [*Maffione*, 1993; *Zaneveld and Pegau*, 1993]. Analytical results are derived on the limiting values of $\bar{\mu}$ both for the case when $r \to 0$ and when $r \to \infty$. We also discuss the case of a finite source. A simple exponential equation is presented as a model for $\bar{\mu}$ which is valid to at least 15 optical lengths from the source. The $\bar{\mu}$ model is used to compute the mean light path, defined by (17), which is then used to accurately calculate the absorption coefficient. Errors in neglecting the increase in the mean light path are investigated.

Approach

The MC model uses standard Monte Carlo techniques for computing photon propagation in an absorbing and scattering medium (see, for example, *Mobley* [1994, chapter 6]). Spherical polar coordinates are most appropriate for describing the radiance distribution L due to an IPS situated at the origin, as shown in Figure 1. In homogeneous water the symmetry of the radiance distribution at all points in space allows L to be specified as a function of one independent angular variable θ' (refer to Figure 1). Along any radial path from the point source, θ' is defined as the angle that the radiance direction vector $\hat{\xi}$ makes with the radial line from the IPS to the point where the radiance is specified. If, for example, a radiometer is pointing directly at the source, it is measuring the radiance in the direction $\theta' = 0$. The symmetry of the problem also allows L to be specified as a function of the distance r from the source; the radial direction from the origin is irrelevant.

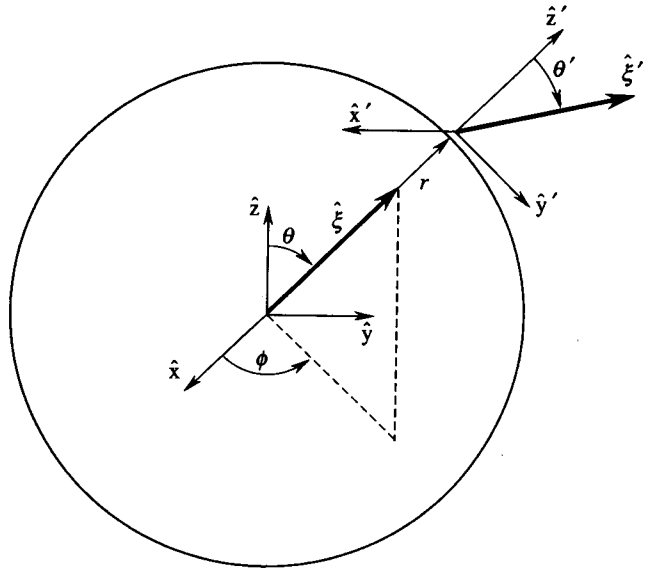

Figure 1. Coordinate system for the Monte Carlo model that computes the radiance distribution due to an isotropic point source at the origin.

Making use of these symmetry properties in the Monte Carlo simulations greatly reduces computation time. Computing the radiance distribution at a point in space does not require counting only those photons which cross that point (strictly speaking, a small area). All of the photons which cross an imaginary sphere of radius r are tallied according to the direction θ' that they are heading when they cross the sphere to compute the radiance distribution $L(r, \theta')$. Because it does not matter where on the sphere the photons cross, by reciprocity it does not matter in which direction the photons are initially launched. A computational step is saved by launching all of the photons in one direction. This simulation is thus analogous to an experiment where the radiance distribution at all points a distance r from a collimated source is measured and then summed or integrated to produce the radiance distribution that would have been measured at a single point a distance r from an isotropic source. The results are identical because an isotropic source is equivalent to a collimated source being pointed in all directions at once.

To simplify the notation, we will henceforth drop the prime on the angular variable θ, keeping in mind that we are

Table 1. Optical Parameters for Monte Carlo Simulations

Type	a, m^{-1}	b, m^{-1}	c, m^{-1}	ω_0, b/c
Deep	0.08	0.08	0.16	0.5
Coast	0.10	0.15	0.25	0.6
Bay	0.30	1.20	1.50	0.8
Milk	0.06	1.14	1.20	0.95

referring to the polar angle in the prime coordinate system shown in Figure 1. Then $\bar{\mu}$ is given by

$$\bar{\mu}(r) = \frac{\int_0^{\pi} L(r, \theta) \cos\theta \sin\theta \, d\theta}{\int_0^{\pi} L(r, \theta) \sin\theta \, d\theta}$$

$$= \frac{\int_0^{\pi/2} L(r, \theta) \cos\theta \sin\theta \, d\theta - \int_{\pi/2}^{\pi} L(r, \theta) |\cos\theta| \sin\theta \, d\theta}{\int_0^{\pi/2} L(r, \theta) \sin\theta \, d\theta + \int_{\pi/2}^{\pi} L(r, \theta) \sin\theta \, d\theta} \tag{5}$$

$$= \frac{E_+(r) - E_-(r)}{E_{0+}(r) + E_{0-}(r)}$$

where the plus and minus subscripts denote the forward and backward hemisphere irradiances, respectively, defined by the limits of integration of the separate terms in the second equation. Because the reduction in computation time by excluding the calculation of the radiance distribution in the backward hemisphere is significant, we chose to compute the radiance distribution only from 0 to $\pi/2$. Our estimation of $\bar{\mu}$,

$$\bar{\mu} \cong \frac{\int_0^{\pi/2} L(\theta) \cos\theta \sin\theta \, d\theta}{\int_0^{\pi/2} L(\theta) \sin\theta \, d\theta} \tag{6}$$

$$= \frac{E_+}{E_{0+}}$$

therefore assumes that $E_+ \gg E_-$ and $E_{0+} \gg E_{0-}$. The fact that the VSFs of ocean water are highly peaked in the forward direction indicates that this ought to be an excellent approximation. Furthermore, measurements [*Honey and Maffione*, 1992; *Maffione*, 1993; *Maffione et al.*, 1991, 1993] show that $E_-/E_+ < 0.01$ for various natural waters. Bear in mind that this is an excellent approximation for irradiances due to an IPS and is not meant to apply to comparisons of downwelling with upwelling irradiances due to solar illumination of the ocean.

For the present study we define four cases which we refer to as deep, coast, bay, and milk. The associated volume absorption, total scattering, and beam attenuation coefficients are listed in Table 1. These values for a, b, and c, respectively, were chosen to represent what could be considered typical, at a wavelength of 530 nm, for clear ocean water, coastal water, bay or harbor water, and extremely turbid water dominated by scattering. The single scattering albedo, $\omega_0 = b/c$, for these four cases range from 0.5 to 0.95, which encompasses nearly all natural water.

Two different volume scattering functions were used to investigate the dependence of the radiance distribution and $\bar{\mu}$ on the VSF. Both VSFs are from *Petzold* [1972], which were measured at 530 nm with a bandwidth of 100 nm; one is referred to as station 8 (AUTEC, test 161, July 13, 1971) and the other as station 11 (HAOCE, August 5, 1971). These two VSFs were chosen because they yield significantly different scattering phase functions for the natural waters measured by Petzold. Figure 2a shows the VSFs, and Figure 2b shows the cumulative scattering probability functions for these two stations. The derivative of the scattering probability function is the scattering phase function. Note that the station 11 VSF has a higher slope than the station 8 VSF, and this higher slope results in a higher photon scattering probability function over all angles.

For each of the four water types given in Table 1, radiance distributions were computed at seven discrete distances from the source corresponding to optical lengths of 0.1, 0.5, 1, 3, 6, 10, and 15. Since the attenuation coefficient c is constant, the optical path length τ is defined as

$$\tau = cr,$$

which is dimensionless. One optical length, $\tau = 1$, represents the distance that a pencil beam of radiance is reduced by a factor e^{-1} due to absorption and scattering of light out of the beam. Throughout this paper, numerical results are given in terms of the optical path length τ, but in the proofs and some discussions we use the radial distance r for clarity. It should be clear that the two variables are easily interchanged.

Theory

Limiting Values of the Average Cosine Due to an IPS

The limit $r \to \infty$. The existence of an asymptotic light field in a homogeneous ocean was first explored mathematically by *Preisendorfer* [1959] and was rigorously proven to exist by *Højerslev and Zaneveld* [1977]. By its definition the asymptotic light field is independent of boundary conditions and is determined solely by the IOPs of the water. Therefore relationships derived for the asymptotic light field apply equally well for an IPS boundary condition as they do for solar, plane-wave illumination. For example, (1) was derived for an IPS boundary condition and becomes (4), derived for the daylight illumination boundary condition, as $r \to \infty$. Without the existence of an asymptotic light field, the equality of (1) and (4) really only proves that

$$\bar{\mu}_{r\infty}/\bar{\mu}_{\infty} = K_{\infty}/K_{r\infty}$$

This ratio is unity because all diffuse attenuation coefficients become equal in the asymptotic limit. Therefore, in the asymptotic limit the average cosines for a homogeneous ocean illuminated by the Sun and embedded with an IPS are equal.

That the asymptotic average cosines are equal allows us to use equations for $\bar{\mu}_{\infty}$ that were derived for the submarine daylight field. For example, the so-called Wilson-Honey relationship [*Wilson*, 1979] for K_{∞}/c, namely,

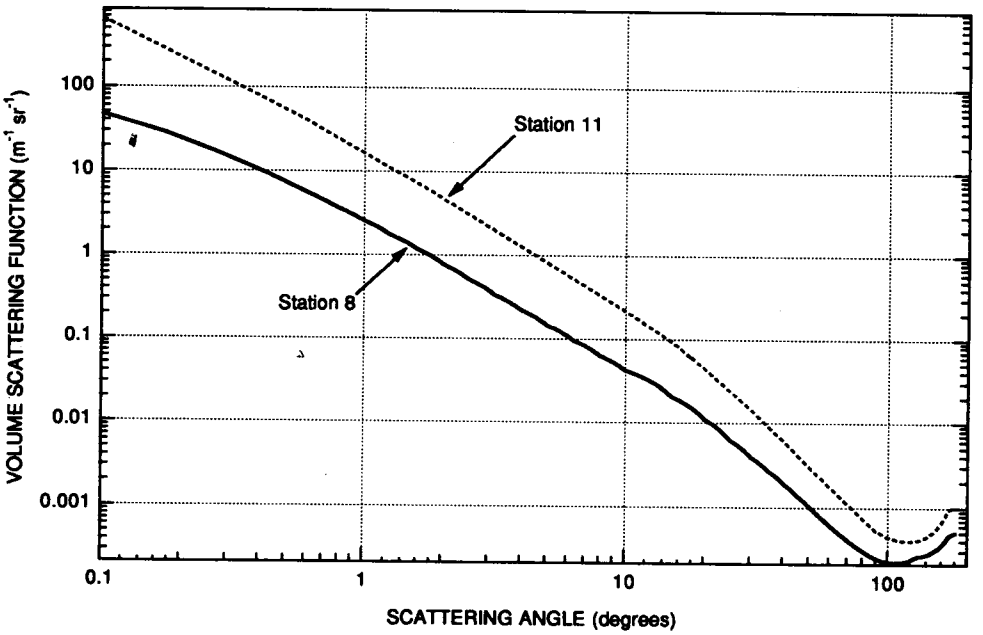

Figure 2a. Volume scattering functions (VSFs) from *Petzold* [1972] used in Monte Carlo simulations. Station 8 is AUTEC, test 161, July 13, 1971; station 11 is HAOCE, August 5, 1971.

$$K_\infty/c = 1 - \tfrac{5}{6}\omega_0$$

can be manipulated using (4) to give

$$\bar{\mu}_\infty = \frac{1-\omega_0}{1-\frac{5}{6}\omega_0}. \tag{7}$$

Zaneveld [1989] used a second-order expansion

$$K_\infty/c = 1 - \gamma_1\omega_0 - \gamma_2\omega_0^2 \tag{8}$$

to fit data from *Prieur and Morel* [1971] and *Timofeeva* [1971] using the coefficients $\alpha_1 = 0.52$ and $\alpha_2 = 0.44$. The expression for $\bar{\mu}_\infty$ using (4) and (8) is

$$\bar{\mu}_\infty = \frac{1-\omega_0}{1-\gamma_1\omega_0-\gamma_2\omega_0^2}. \tag{9}$$

It is interesting to note that although K_∞/c does not depend strongly on the second-order term, $\bar{\mu}_\infty$ does. We performed a least squares regression using (9) with data from C. D.

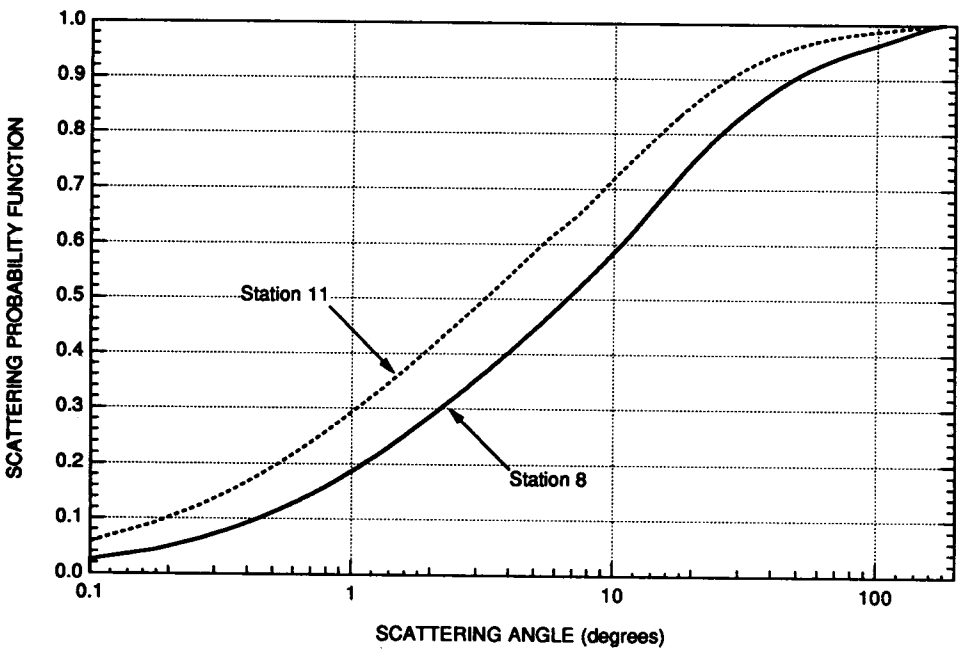

Figure 2b. Scattering probability functions of the station 8 and station 11 VSFs.

Table 2. Coefficients for $\bar{\mu}_\infty$ Regression to Equation (9)

Coefficients	Empirical, *Zaneveld* [1989]	Eigenmatrix Method[a] Station 8	Eigenmatrix Method[a] Station 11
γ_1	0.52	0.532	0.666
γ_2	0.44	0.379	0.280

[a] *Mobley* [1994].

Mobley (private communication, 1994) that he computed with an eigenmatrix method [*Mobley*, 1994; *Mobley et al.*, 1993]. Mobley ran the same cases (refer to Table 1) with the two *Petzold* [1972] VSFs used in our simulations. Table 2 gives the coefficients and Figure 3 shows the resulting $\bar{\mu}_\infty$ curves for Wilson-Honey, [*Wilson*, 1979], *Zaneveld* [1989], and *Mobley* [1994].

The limit $r \to 0$. To derive this limit of $\bar{\mu}$, we must be able to specify the radiance distribution as $r \to 0$. Since the area of a point source is zero, its radiance is undefined. This does not, however, prevent us from considering the radiance distribution due to a point source or the radiance at $\theta = 0$. Conceptually, we may think of the area of the source to be the area that an infinitesimal solid angle subtends at r. As $r \to 0$, the area decreases as r^2 and likewise goes to zero. The radiance distribution must become more and more sharply peaked since the fraction of photons heading in the direction $\theta = 0$ must greatly increase over the fraction that are scattered into other angles as $r \to 0$. This distribution will approach a delta function because the radiance at $r = 0$ becomes infinite since the subtended area goes to zero. For the same reason, the radiance at all other angles goes to zero. Therefore we postulate or assert that the radiance distribution approaches some delta sequence $\delta_n(\theta)$ such that as $r \to 0$, $n \to \infty$, and $\delta_n(\theta) \to \delta(\theta)$, the Dirac delta function. Specifically,

$$\lim_{r\to 0} L(r, \theta) = \lim_{n\to\infty} \frac{I_s}{r^2}\,\delta_n(\theta) = \frac{I_s}{r^2}\,\delta(\theta) \tag{10}$$

where I_s is the (finite) radiant intensity of the IPS.

Starting with the definition of $\bar{\mu}$ as given by (5) and applying (10), we see that

$$\lim_{r\to 0} \bar{\mu}(r) = \lim_{r\to 0} \frac{\int_0^\pi L(r, \theta) \cos\theta \sin\theta\, d\theta}{\int_0^\pi L(r, \theta) \sin\theta\, d\theta}$$

$$= \frac{\int_0^\pi \left[\lim_{r\to 0} L(r, \theta)\right] \cos\theta \sin\theta\, d\theta}{\int_0^\pi \left[\lim_{r\to 0} L(r, \theta)\right] \sin\theta\, d\theta}$$

$$= \frac{\int_0^\pi \delta(\theta) \cos\theta \sin\theta\, d\theta}{\int_0^\pi \delta(\theta) \sin\theta\, d\theta} \tag{11}$$

$$= \frac{\cos(0) \sin(0)}{\sin(0)}$$

Since this limit evaluates to 0/0, we may apply l'Hôspital's rule, which gives

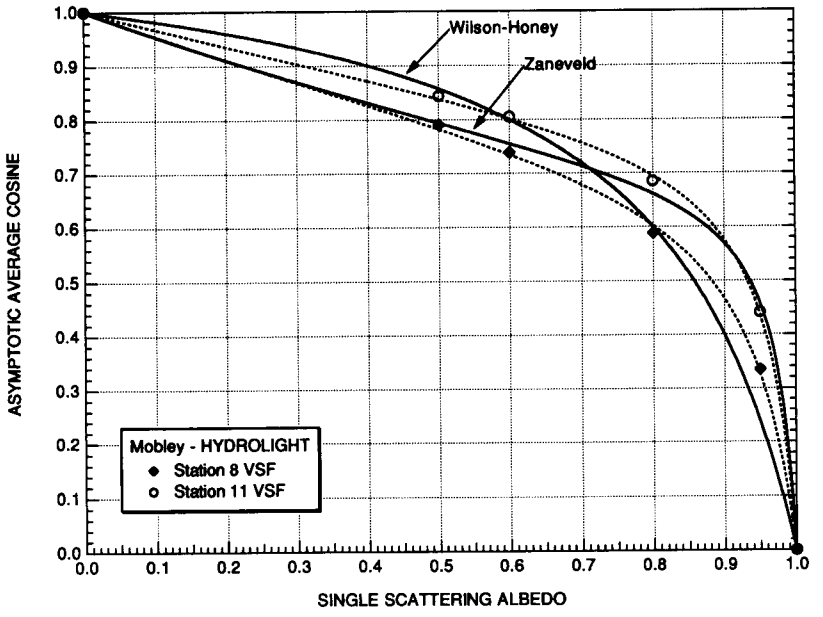

Figure 3. Asymptotic average cosine from the Wilson-Honey [*Wilson*, 1979] and *Zaneveld* [1989] equations compared with $\bar{\mu}_\infty$ values computed with the *Mobley* [1994] eigenmatrix method using the station 8 and 11 VSFs. The dotted lines were computed from a regression using (9).

$$\lim_{\theta\to 0}\frac{\cos(\theta)\sin(\theta)}{\sin(\theta)} = \lim_{\theta\to 0}\frac{\cos^2(\theta)-\sin^2(\theta)}{\cos(\theta)}$$

$$= 1. \quad \blacksquare$$

Therefore $\bar{\mu}(0) = 1$ for an isotropic point source.

Limit for a finite source. In practice, isotropic point sources are approximated by finite diffuse (quasi) isotropic sources [*Brown et al.*, 1991]. If the radius of the source is R, then the question to be addressed is as follows: What is the limiting value of $\bar{\mu}$ as $r \to R$? Since a diffuse isotropic source is a plane Lambertian source at its surface, then from (5) and (6) we have,

$$\bar{\mu}(R) = \lim_{r\to R}\bar{\mu}(r)$$

$$= \lim_{r\to R}\frac{\int_0^{\pi} L(r,\theta)\cos\theta\sin\theta\,d\theta}{\int_0^{\pi} L(r,\theta)\sin\theta\,d\theta}$$

$$= \frac{L_s\int_0^{\pi/2}\cos\theta\sin\theta\,d\theta - \int_{\pi/2}^{\pi} L(R,\theta)\cos\theta\sin\theta\,d\theta}{L_s\int_0^{\pi/2}\sin\theta\,d\theta + \int_{\pi/2}^{\pi} L(R,\theta)\sin\theta\,d\theta}$$

$$= \frac{L_s\frac{1}{2} - E_-(R)}{L_s + E_{0-}(R)} \cong \frac{1}{2} \tag{12}$$

where L_s is the radiance of the Lambertian source and we have assumed that $L_s \gg E_-(R), E_{0-}(R)$, which is clearly true for any realistic volume scattering function. In taking L_s out of the integral we have also assumed that $R \ll 1/c$. Essentially, we are assuming that the water optical properties and the relative size of the source is such that, at very close distances to the source, it will appear as a plane Lambertian source in air, where the proof holds exactly.

Now consider what happens to $\bar{\mu}$ in the region from the surface of the source to about one optical length ($\tau = 1$). The source subtends a half angle at r given by $\sin\alpha = R/r$. Then $\bar{\mu}$ may be written as

$$\bar{\mu}(r)$$

$$= \frac{\int_0^{\alpha} L(r,\theta)\cos\theta\sin\theta\,d\theta + \int_{\alpha}^{\pi} L(r,\theta)\cos\theta\sin\theta\,d\theta}{\int_0^{\alpha} L(r,\theta)\sin\theta\,d\theta + \int_{\alpha}^{\pi} L(r,\theta)\sin\theta\,d\theta}$$

$$\cong \frac{L_s\int_0^{\alpha}\cos\theta\sin\theta\,d\theta + \int_{\alpha}^{\pi} L(r,\theta)\cos\theta\sin\theta\,d\theta}{L_s\int_0^{\alpha}\sin\theta\,d\theta + \int_{\alpha}^{\pi} L(r,\theta)\sin\theta\,d\theta} \tag{13}$$

$$= \frac{L_s\frac{\sin^2\alpha}{2} + \int_{\alpha}^{\pi} L(r,\theta)\cos\theta\sin\theta\,d\theta}{L_s 2\sin^2(\alpha/2) + \int_{\alpha}^{\pi} L(r,\theta)\sin\theta\,d\theta}$$

which is clearly an excellent approximation since the differential path to all points on the source is small and thus L_s is nearly constant with angle. In the region $r < 1/c$ it should also be a very good approximation to neglect the second terms in the numerator and denominator since α will be large and the radiance of the source dominates the radiance distribution. Therefore

$$\bar{\mu} \cong \frac{\sin^2\alpha}{4\sin^2(\alpha/2)} = \frac{(R/r)^2}{2\{1-\sqrt{1-[(R/r)^2]}\}} \tag{14}$$

This function is plotted in Figure 4 with R/r as the independent variable. It is evident that although $\bar{\mu} = 0.5$ at $r = R$, it rapidly approaches unity in a short distance from the surface of the source. At distances farther than $R/r = 0.1$, $\bar{\mu}$ will decrease in nearly the same fashion as it would for a point source, and the two cases will rapidly become indistinguishable as $r \to \infty$. Experimentally then, where finite diffuse isotropic sources are used, the average cosine of the light field will be nearly identical to the IPS $\bar{\mu}$ at distances greater than, say, one optical length as long as the radius of the source is small compared to $1/c$.

The Mean Light Path and the Absorption Coefficient

If there were no scattering of light in a homogeneous ocean, then the irradiance flowing outward from the source would attenuate geometrically as $1/r^2$ and exponentially according to Beer's law as $\exp(-ar)$. More precisely,

$$E(r) = E_+(r) = \frac{\Phi_s}{4\pi r^2}\exp(-ar), \tag{15}$$

showing explicitly that the net irradiance E equals the outward flowing irradiance E_+ since there is no scattering, i.e., $E_- = 0$. Φ_s is the radiant flux of the source.

Scattering increases the geometric distance photons travel, thereby increasing the probability of photon absorption. An emitted photon that makes it to a radial distance r after one or more scattering events will have actually traveled a total distance $r + \delta r$. To compute the irradiance at r, all photon paths to that point would have to be accounted for and the resulting calculation would be unwieldy, but *Maffione et al.* [1993] showed that the net irradiance is given exactly by

$$E(r) = \frac{\Phi_s}{4\pi r^2}\exp(-a\bar{r}) \tag{16}$$

where

$$\bar{r} = \int_0^r \frac{dr'}{\bar{\mu}(r')} \tag{17}$$

is defined as the mean light path. So we see that $\bar{r}$, which depends solely on the average cosine, magically takes into account all of the photon paths when computing net irradiance at a distance r from the IPS.

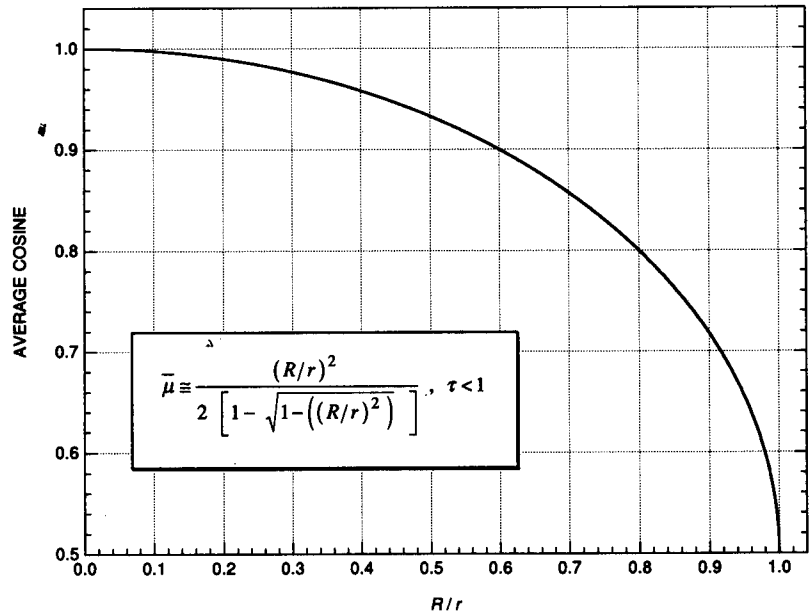

Figure 4. The average cosine within one optical length of a finite isotropic source where the radius of the source is one tenth of an optical length.

Comparing (15) with (16) implies that we may write $\bar{r} = r + \overline{\delta r}$, where $\overline{\delta r}$ is defined as the mean increase in the light path due to scattering. The import of $\overline{\delta r}$ is that it applies to any geometry, yet nearly all methods for measuring the absorption coefficient [*Pegau et al.*, this issue] neglect it and use the geometric distance, analogous to r, for the path length. The mathematical formulation of the IPS method for determining a, summarized by (16) and (17), provides an exact expression for the mean increase in the light path, namely,

$$\overline{\delta r}(r) = \int_0^r \left[\frac{1}{\bar{\mu}(r')} - 1\right] dr' \qquad (18)$$

which we investigate here with the MC model.

Results

Comparison of Simulations With Measured PSFs

Measurements of the PSF at Lake Pend Oreille, Idaho, with both plane Lambertian and isotropic sources, provided us an opportunity to compare the MC model to measurements in natural water. The measurements were conducted as part of the ONR sponsored optical closure experiment in April–May 1992. The experimental arrangement is described by *Maffione et al.* [1991, 1993]. Briefly, a light source [*Brown et al.*, 1991] is lowered into the water, and images of the source are recorded by an integrating CCD camera [*Voss and Chapin*, 1990]. The electronic camera is lowered to some depth, and the distance between the source and camera are varied by changing the depth of the source. During the Lake Pend Oreille experiment we used a 50-mm focal-length lens and a 532-nm interference filter (10-nm bandwidth) with the camera. This arrangement provided measurements of the PSF out to nearly 20°, although light levels were usually noise limited by 15°.

The light source arrangement allowed us to interchange a flat diffuser with a diffusing globe. The flat diffuser created a cosine (i.e., plane Lambertian) source with a diameter of 3.8 cm. The diffusing globe created an isotropic source with a diameter of 12.7 cm. Most measurements at Lake Pend Oreille were made with the isotropic source. Occasionally, we made measurements with the cosine source to see how these PSFs compared with the isotropic-source PSFs. The advantage of using the flat diffuser is that all of the light emitted by the light source is initially directed into the forward hemisphere, toward the camera, allowing us to measure the radiance distribution at larger angles and at farther distances from the source than we could when all of the light is directed isotropically.

On May 6 a series of PSFs were measured using the isotropic source with the camera held at a 60-m depth. When the run was complete, the system was immediately hauled to the surface and the diffusing globe was replaced with the flat diffuser, creating a cosine source. Then another series of PSF measurements were made with the camera at the same depth. The absorption and beam attenuation coefficients were estimated with the IPS method [*Maffione et al.*, 1991, 1993]. At 60 m they were $a = 0.12\ \mathrm{m}^{-1}$ and $c = 0.40\ \mathrm{m}^{-1}$ at 532 nm. Thus the single scattering albedo was $\omega_0 = 0.70$. These optical properties most closely match our "coast" PSF simulations (refer to Table 1). Figures 5a–5d show comparison plots of the measured PSFs with the simulated coast PSFs at one, three, six, and ten optical lengths for the simulated data. These optical path lengths roughly correspond to the optical path lengths of the measured PSFs. The isotropic source PSF is missing in Figure 5d because there was not enough measurable light at this distance. The PSF units are arbitrary and were scaled to adjust the vertical height of the curves for better comparison. We are not interested in the absolute magnitudes, only the shapes of the PSFs, which are not affected by our scaling. The scales of the four plots are identical so that the slopes and their changes with distance can more easily be compared.

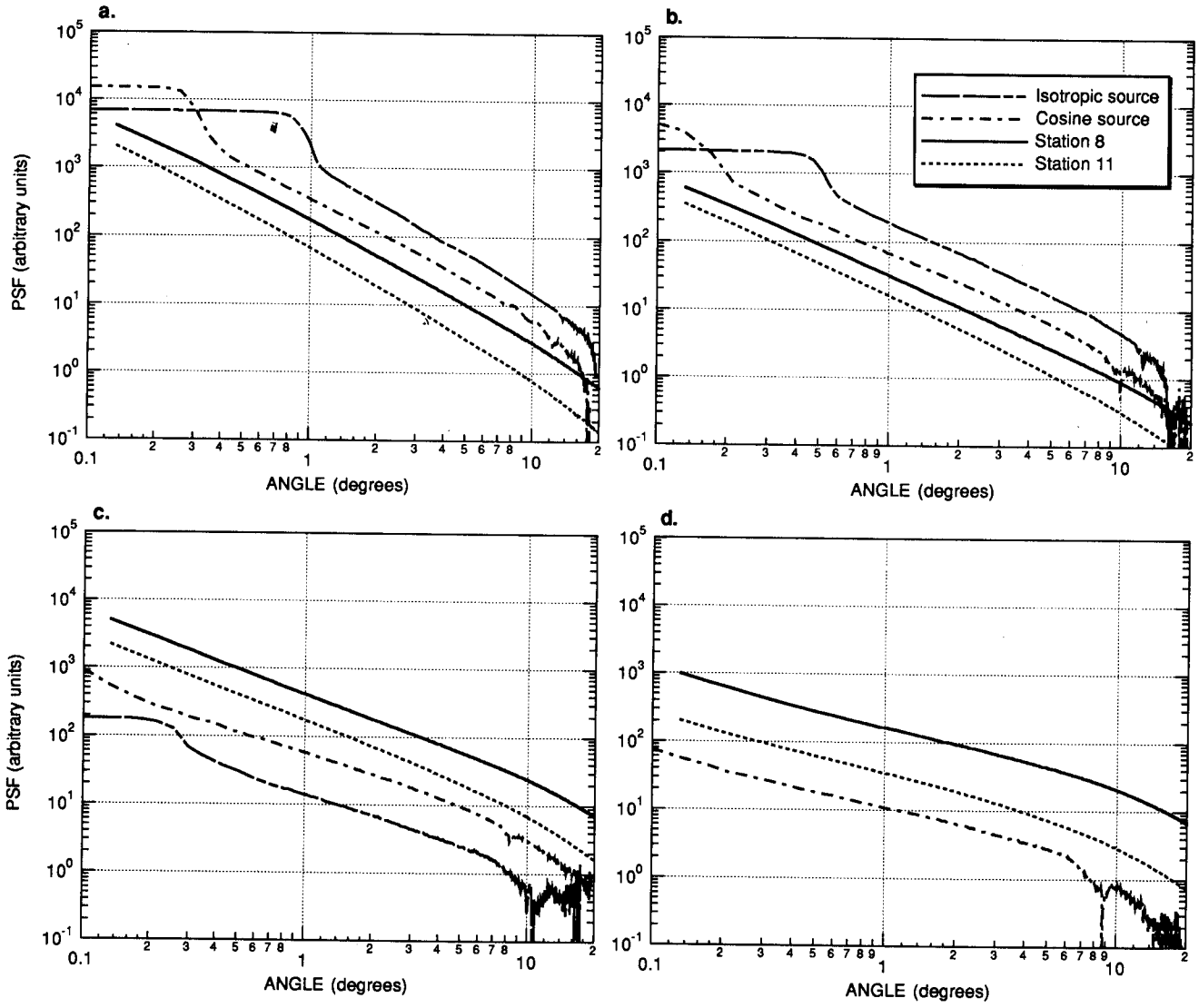

Figure 5. Comparisons of the Monte Carlo radiance distributions or point spread functions (PSFs) and the measured PSFs at Lake Pend Oreille during the optical closure experiment. (a) Approximately one optical length from the source; (b) approximately three optical lengths from the source; (c) approximately six optical lengths from the source; and (d) approximately 10 optical lengths from the source.

As the distance from the source is increased, the slope of the PSF will decrease due to multiple scattering of photons into larger angles that were initially headed at smaller, forward angles. Figures 5a–5d clearly show the decreasing slopes at greater ranges for both the modeled and measured PSFs. The horizontal portion of the measured PSFs are the sources themselves. The extremely sharp drop-off is an edge effect caused by the sharp transition in the radiance distribution from directly transmitted plus scattering light to purely scattered light. For our comparison we are interested in the portion of the PSF away from source and edge effects.

At a fixed distance from the source the slope of the PSF will be primarily dependent on the VSF and the ω_0 of the water. The station 11 VSF yields higher PSF slopes than the station 8 VSF, as expected, because the former VSF has a steeper slope than the latter (refer to Figure 2a). A steeper slope means a higher scattering probability function (refer to Figure 2b) which implies that a greater fraction of scattered photons are contained within the smaller scattering angles causing the PSF to decrease faster with increasing radiance angle. The slopes of the PSFs were computed at a radiance angle of about 5° and are plotted in Figure 6 as a function of optical path length. The slope of the PSF was computed by a linear regression on a log-log scale. In general, the measured PSF slopes fall between the model PSF slopes for the two VSFs used in the simulations. If the slopes at 3τ for the measured PSFs are ignored, the trends for the change in slopes with optical path length are fairly similar. The anomalous slopes at 3τ are probably a measurement artifact since linear trends were found when these plots were made using slopes computed at angles other than 5°. It is not the intent here to present an analysis of PSF slopes but rather to demonstrate that the model gives physically reasonable PSFs.

Model of the Average Cosine

The average cosine was computed with (6) at the seven optical path lengths for each water type (refer to Table 1) and

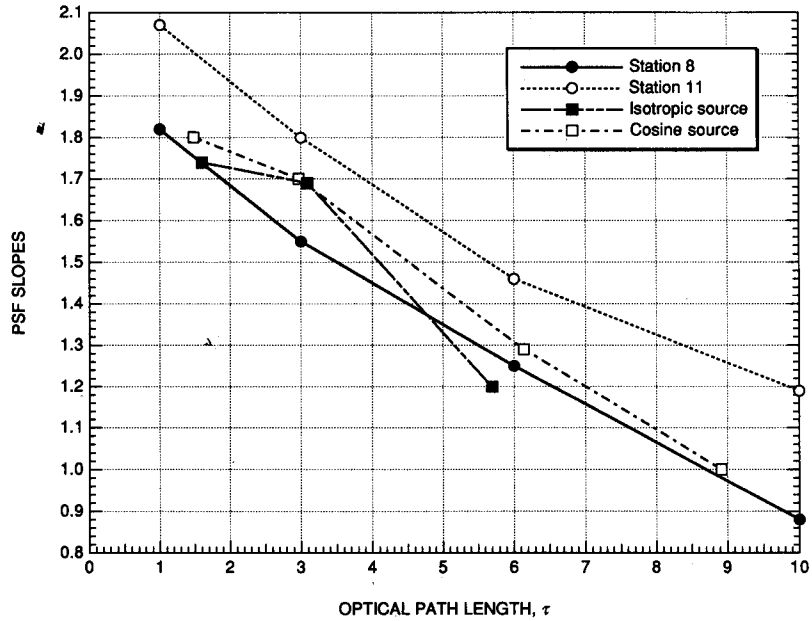

Figure 6. Comparison of PSF slopes from measurements at Lake Pend Oreille with the Monte Carlo "coast" runs.

for the two *Petzold* [1972] VSFs (stations 8 and 11). Figure 7 shows the results for station 11. We found that $\bar{\mu}$ fit the exponential equation

$$\bar{\mu}(\tau) = k_0 + k_1 \exp(-k_2\tau) \tag{19}$$

quite well for all of the simulations. The regression coefficients, k_0, k_1, k_2, for all of the cases we studied are given in Table 3. Note that $k_0 + k_1$ sums almost exactly to one in all cases, as it should by our proof that $\bar{\mu} \to 1$ as $\tau \to 0$. We did not constrain the regression to do so.

A fortunate coincidence of (19) is that it can be integrated to give analytic solutions to (17) and (18). The solutions are

$$\bar{\tau} = \frac{\tau}{k_0} + \frac{1}{k_0 k_2} \ln[\bar{\mu}(\tau)] \tag{20}$$

$$\overline{\delta\tau} = \tau\left(\frac{1}{k_0} - 1\right) + \frac{1}{k_0 k_2} \ln[\bar{\mu}(\tau)] \tag{21}$$

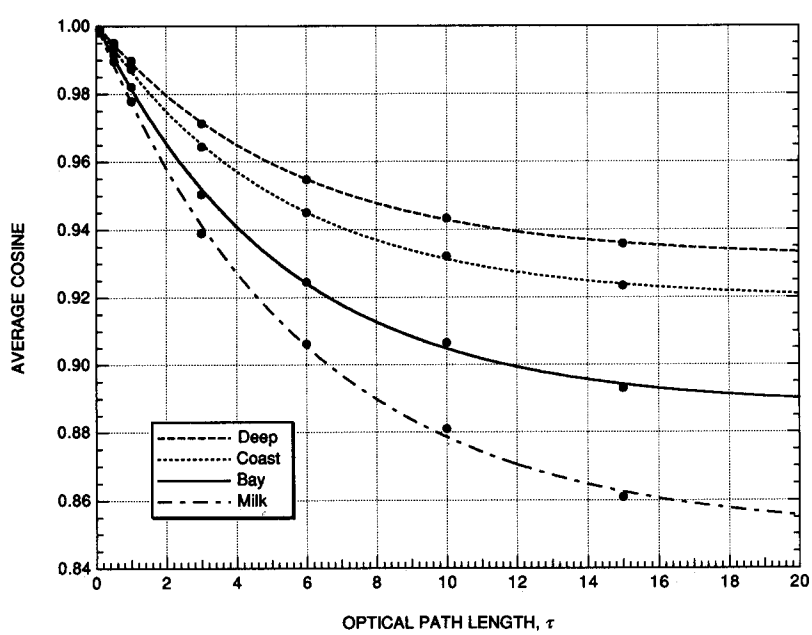

Figure 7. The average cosine as a function of optical path length from an isotropic point source (IPS) computed from the station 11 VSF simulations. Solid curves were determined from a regression to (19).

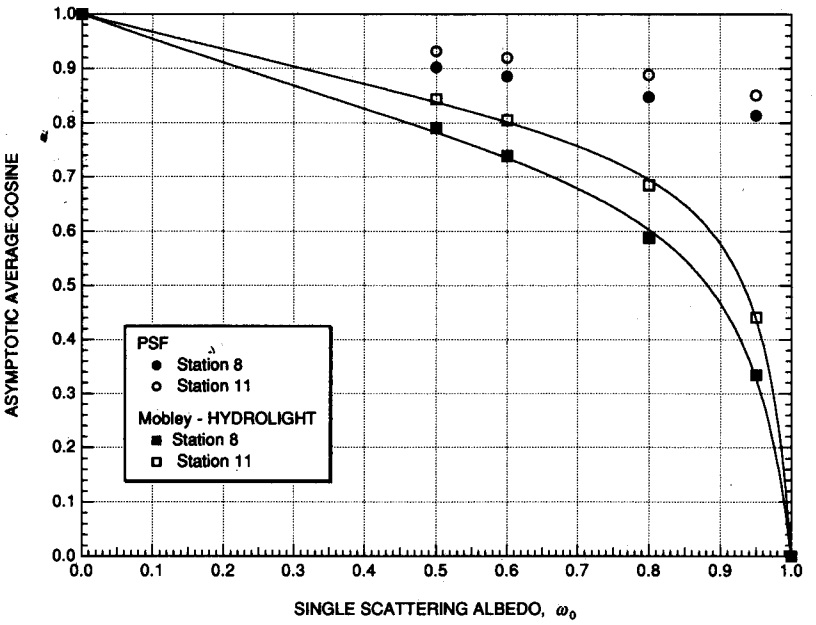

Figure 9. Comparison of average cosines from Monte Carlo simulations at 15 optical lengths with asymptotic average cosines from eigenmatrix computations.

al., 1991, 1993]. Taking the natural logarithm of (16) and rearranging gives

$$\ln [r^2 E(r)] = \ln \left(\frac{\Phi_s}{4\pi} \right) - a\bar{r} \qquad (22a)$$

$$\cong \ln \left(\frac{\Phi_s}{4\pi} \right) - ar. \qquad (22b)$$

The slope of a linear regression of the measurements of $E(r)$ to (22a) yields the absorption coefficient, assuming $\bar{r}(r)$ is known. In practice, $\bar{r}(r)$ is not known and (22b) is used to estimate a. As we showed above, to a very good approximation, especially near the source, $\bar{r} \cong r$.

From our simulations we can now estimate $\bar{r}(r)$ using (20) and investigate the errors in estimating a using (22b). Also, because the MC model uses a known input value of a, we

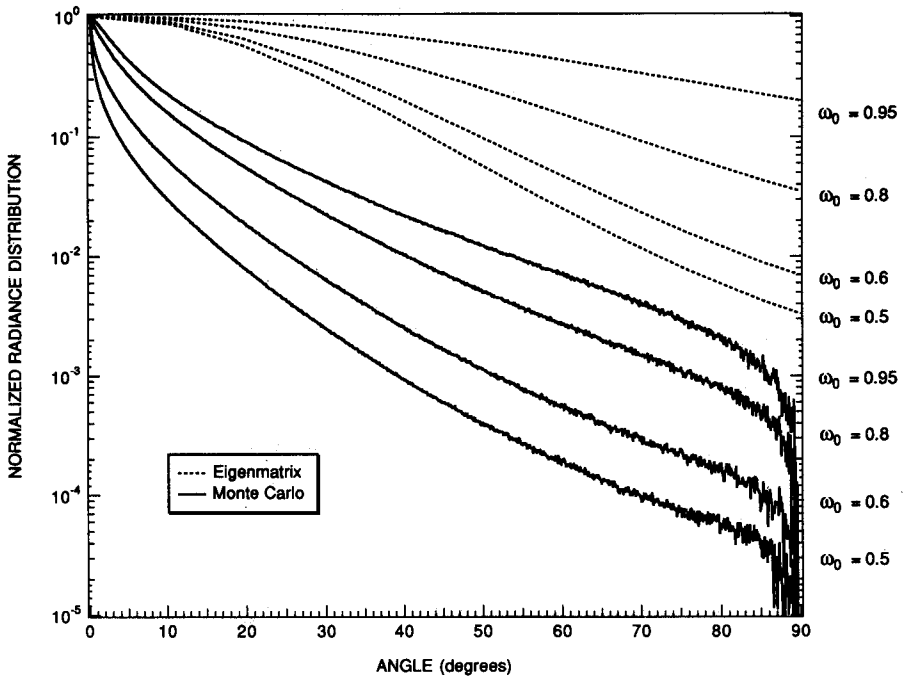

Figure 10. Comparison of normalized radiance distributions from Monte Carlo simulations at 15 optical lengths with asymptotic radiance distributions from eigenmatrix computations.

Table 4a. Estimates of Absorption Coefficients and Errors (*Petzold* [1972] Station 8 VSF)

		Without $\bar{\mu}$ Correction		With $\bar{\mu}$ Correction	
Type	True a, m^{-1}	Estimated a, m^{-1}	Percent Error	Estimated a, m^{-1}	Percent Error
Deep	0.080	0.0892	11	0.0807	0.9
Coast	0.100	0.115	15	0.102	2.0
Bay	0.300	0.372	24	0.335	12
Milk	0.060	0.0807	34	0.070	17

Table 4b. Estimates of Absorption Coefficients and Errors (*Petzold* [1972] Station 11 VSF)

		Without $\bar{\mu}$ Correction		With $\bar{\mu}$ Correction	
Type	True a, m^{-1}	Estimated a, m^{-1}	Percent Error	Estimated a, m^{-1}	Percent Error
Deep	0.080	0.0848	6.0	0.0793	0.9
Coast	0.100	0.108	8.0	0.0996	0.4
Bay	0.300	0.336	12	0.316	5.3
Milk	0.060	0.0708	18	0.0646	7.7

can check the accuracy of the MC model and the $\bar{\mu}$ model (19) by estimating a with (22a) since this equation is exact. The results are summarized in Tables 4a and 4b, where the last columns give the percent error in estimating a with (22a). These errors are due to errors in both the MC model and the $\bar{\mu}$ model together since the $\bar{\mu}$ model was needed to compute $\bar{r}(r)$. The fourth columns give the percent error in estimating a with (22b), which neglects the mean light-path increase $\overline{\delta\tau}$. These errors, however, include the errors due to the MC and $\bar{\mu}$ models as well as the errors in using the approximation (22b). Therefore the difference between the errors in columns 4 and 6 is a better indicator of the errors due to using (22b) for estimating a. Ignoring the milk runs, which are not realistic for natural waters, the largest error is then about 12% (bay, station 8 VSF) and the smallest is about 5% (deep, station 11 VSF).

One observation of these results is that the error in estimating a is a strong function of both ω_0 and the VSF. That the errors should be strongly related to ω_0 is expected, but the strong dependence on the VSF is somewhat surprising. The errors roughly double between the station 11 VSF and the station 8 VSF, yet the scattering probability functions do not differ that greatly between the two VSFs (refer to Figure 2b). Evidently, however, this difference does have a significant effect on the mean light path. Figure 11 shows the differences in the increase in the mean light paths, $\overline{\delta\tau}$ (station 8) − $\overline{\delta\tau}$ (station 11). Comparing this to Figure 8 shows that the change in $\overline{\delta\tau}$ is over half the magnitude of $\overline{\delta\tau}$ for the station 11 VSF.

Conclusions

The radiance distribution due to an isotropic point source embedded in the ocean can, in theory, be inverted to yield all of the inherent optical properties of the medium. Approximations have been developed by *Sorenson and Honey* [1968] and *Wells* [1969]. Sorenson and Honey's approximations can be used to estimate the absorption, attenuation, and backward scattering coefficients. Wells' paraxial approximation can be analytically inverted to yield the volume scattering function in the small-angle limit. The accuracy of these approximations depends on the shape of the volume scattering function as well as the distance to the light source. The only known exact solution for an IOP derived from an IPS light field was presented by *Maffione et al.* [1993]. They derived the absorption coefficient by transforming *Gershun*'s [1936] equation to spherical coordinates. Their derivation showed that the average cosine $\bar{\mu}$ was fundamental to describing how scattering increases the optical path length and thus the probability of photon absorption.

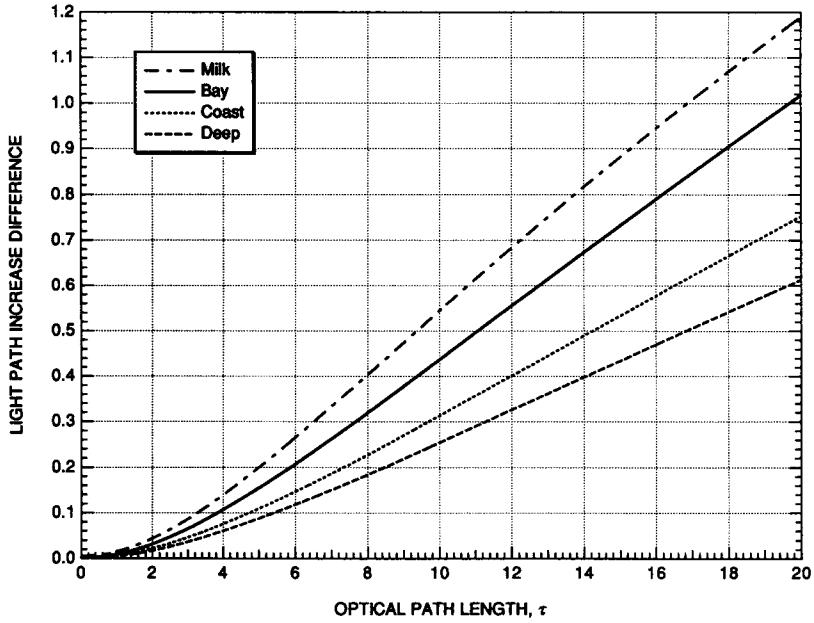

Figure 11. Differences in the mean light-path increase from the station 8 and 11 VSFs.

A Monte Carlo model that computes the IPS radiance distribution was compared with point spread functions measured in Lake Pend Oreille, Idaho [*Maffione*, 1993]. MC simulations using volume scattering functions from *Petzold* [1972] compared quite well with the measured PSFs (Figures 5a–5d). The slopes of the measured PSFs fell within the slopes of the simulated PSFs (Figure 6).

For homogeneous water the asymptotic radiance distribution is only a function of the IOPs and independent of the boundary conditions [*Preisendorfer*, 1959; *Højerslev and Zaneveld*, 1977]. Given the same IOPs, the asymptotic light field due to an embedded IPS is thus identical to that for an ocean illuminated by solar, plane-wave radiation. Comparing the MC results at 15 optical lengths from the source to eigenmatrix calculations of the asymptotic daylight field [*Mobley*, 1994] showed that 15 optical lengths is nowhere near the asymptotic limit for an IPS light field, even for the murkiest of waters ($\omega_0 = 0.95$). Using the eigenmatrix results and a model for the asymptotic $\bar{\mu}$ presented by *Zaneveld* [1989], new coefficients for the model were computed that were shown to depend on the VSF (Table 2).

By describing the IPS radiance distribution as a delta sequence near the source, we proved that $\bar{\mu} \to 1$ as $r \to 0$. For a finite diffuse isotroptic source we showed that $\bar{\mu} \to 1/2$ at the surface of the source. If $R \ll 1/c$, where R is the radius of the source and c is the attenuation coefficient, then $\bar{\mu}$ rapidly approaches unity very near the surface, and at distances beyond one optical length $1/c$, it behaves essentially as it would for an IPS. On the basis of our MC simulations we developed a simple analytic model, (19), for $\bar{\mu}$ valid out to at least 15 optical lengths from the source. This model can be used to compute the mean light path, (17), and the increase in the mean light path, (18), due to scattering. The analytic solutions to (17) and (18) based on the model are given by (20) and (21), respectively.

Sorenson and Honey [1968] argued that the absorption coefficient a could be estimated using (22b) which does not depend on the increase in the mean light path due to scattering and hence assumes $\bar{\mu} = 1$. The exact result, (22a), was derived by *Maffione et al.* [1993] and does depend on the true value of $\bar{\mu}$. Our model for $\bar{\mu}$, (19), showed that the errors in neglecting the increase in the mean light path due to scattering are, for nearly all natural waters, between 5% and 12% of the true value of a.

Notation

a absorption coefficient, m^{-1}.
b total scattering coefficient, m^{-1}.
c beam attenuation coefficient, m^{-1}.
E net vertical irradiance, W m^{-2}.
E_r net radial irradiance, W m^{-2}.
E_0 scalar irradiance, W m^{-2}.
K diffuse attenuation coefficient for net vertical irradiance, m^{-1}.
K_∞ asymptotic diffuse attenuation coefficient, m^{-1}.
K_r diffuse attenuation coefficient for net radial irradiance, m^{-1}.
L radiance, W m^{-2} sr^{-1}.
ω_0 single scattering albedo.
$\bar{\mu}$ average cosine.
$\bar{\mu}_\infty$ asymptotic average cosine.
$\bar{\mu}_r$ radial average cosine.
r geometric linear distance.
$\bar{r}$ mean light path.
τ optical path length.

Acknowledgments. We thank Curt Mobley for several useful comments on the draft of this paper and for providing simulated data from his numerical model, HYDROLIGHT. We are grateful to Ken Voss for the use of his point spread function camera during the Lake Pend Oreille experiment and for some stimulating discussions of this work. Others who provided valuable assistance in making the PSF measurements at Lake Pend Oreille were Dick Honey, Al Chapin, and Alan Weidemann. We gratefully acknowledge the support of the Ocean Optics Program at the Office of Naval Research. J. Jaffe at Scripps was supported under grants N00014-93-1138, N00014-90-J-1275, and N00014-94-1-0087.

References

Brown, R. A., R. C. Honey, and R. A. Maffione, Isotropic light source for underwater applications, *Proc. SPIE Int. Soc. Opt. Eng.*, *1537*, 147–150, 1991.

Gershun, A. A., The light field, *J. Math. Phys.*, *18*, 51–151, 1936.

Højerslev, N. K., and J. R. V. Zaneveld, A theoretical proof of the existence of the submarine asymptotic daylight field, *Rep. 34*, Inst. of Phys. Oceanogr., Univ. of Copenhagen, Copenhagen.

Honey, R. C., and R. A. Maffione, Measurement of the optical backscatter coefficient in ocean water, paper presented at Aquatic Sciences Meeting, Am. Soc. of Limnol. and Oceanogr., Santa Fe, N. M., February 1992.

Jaffe, J. S., Validity and range of linear approximations in underwater imaging, *Appl. Opt.*, in press, 1995.

Maffione, R. A., Results of inherent- and apparent-optical-property measurements at Lake Pend Oreille, *Annu. Meet. Tech. Dig.*, *4*, Opt. Soc. of Am., Washington, D. C., 1993.

Maffione, R. A., and R. C. Honey, Results of in-situ closure measurements over long-pathlengths in the ocean, *Annu. Meet. Tech. Dig.*, *17*, Opt. Soc. of Am., Washington, D. C., 1991.

Maffione, R. A., R. C. Honey, and R. A. Brown, Experiment for testing the closure property in ocean optics, *Proc. SPIE Int. Soc. Opt. Eng.*, *1537*, 115–126, 1991.

Maffione, R. A., K. J. Voss, and R. C. Honey, Measurement of the spectral absorption coefficient in the ocean with an isotropic source, *Appl. Opt.*, *32*, 3273–3279, 1993.

Mertens, L. E., and F. S. Replogle Jr., Use of the point spread function for analysis of imaging systems in water, *J. Opt. Soc. Am.*, *67*, 1105–1117, 1977.

Mobley, C. D., *Light and Water: Radiative Transfer in Natural Waters*, 592 pp., Pergamon, Tarrytown, N. Y., 1994.

Mobley, C. D., B. Gentili, H. R. Gordon, Z. Jin, G. W. Kattawaar, A. Morel, P. Reinersman, K. Stamnes, and R. H. Stavn, Comparison of numerical models for computing underwater light fields, *Appl. Opt.*, *32*, 7484–7504, 1993.

Pegau, W. S., et al., A comparison of methods for the measurement of the absorption coefficient in natural waters, *J. Geophys. Res.*, this issue.

Petzold, T. J., Volume scattering functions for selected ocean waters, *Rep. SIO Ref. 72-78*, 79 pp., Scripps Inst. of Oceanogr., La Jolla, Calif., 1972.

Preisendorfer, R. W., Theoretical proof of the existence of characteristic diffuse light in natural waters, *J. Mar. Res.*, *18*, 1–9, 1959.

Prieur, L., and A. Morel, Etude théoretique du régime asymptotique: Relations entre charactéristiques optiques et coefficient d'extinction relatif a la pénétration de la lumiére du jour, *Cah. Oceanogr.*, *23*, 35–48, 1971.

Sorenson, G., and R. C. Honey, Instrumentation for measuring visibility-limiting characteristics of sea water, *Proc. Soc. Photo Opt. Instrum. Eng.*, *12*, 115–122, 1968.

Timofeeva, V. A., Optical characteristics of turbid media of the sea-water type, *Izv. Acad. Sci. USSR Atmos. Oceanic Phys.*, Engl. Transl., *7*, 863–865, 1971.

Voss, K. J., and A. L. Chapin, Measurement of the point spread function in the ocean, *Appl. Opt.*, *29*, 3638–3642, 1990.

Wells, W. H., Loss of resolution in water as a result of multiple small-angle scattering, *J. Opt. Soc. Am.*, *59*, 64–72, 1969.

Wilson, W. H., Spreading of light beams in ocean water, *Proc. Soc. Photo Opt. Instrum. Eng.*, *208*, 115–122, 1979.

Zaneveld, J. R. V., An asymptotic closure theory for irradiance in the sea and its inversion to obtain the inherent optical properties, *Limnol. Oceanogr.*, *34*, 1442–1452, 1989.

Zaneveld, J. R. V., and W. S. Pegau, Overview of the optical closure experiment at Lake Pend Oreille, *Annu. Meet. Tech. Dig.*, *4*, Opt. Soc. of Am., Washington, D. C., 1993.

J. S. Jaffe, Marine Physics Laboratory, Scripps Institution of Oceanography, University of California, La Jolla, CA 92093. (e-mail: jules@fishtv.ucsd.edu)

R. A. Maffione, SRI International, 333 Ravenswood Avenue, Menlo Park, CA 94025. (e-mail: robert_maffione@qm.sri.com)

(Received April 25, 1994; revised November 23, 1994; accepted December 12, 1994.)